NATIONAL ADVISORY COMMITTEE FOR AERONAUTICS

TECHNICAL NOTE 3183

MINIMUM-WAVE-DRAG AIRFOIL SECTIONS FOR ARROW WINGS

By Morton Cooper and Frederick C. Grant

Langley Aeronautical Laboratory
Langley Field, Va.

Washington
May 1954

NATIONAL ADVISORY COMMITTEE FOR AERONAUTICS

TECHNICAL NOTE 3183

MINIMUM-WAVE-DRAG AIRFOIL SECTIONS FOR ARROW WINGS

By Morton Cooper and Frederick C. Grant

SUMMARY

A linearized theoretical analysis has been made to determine minimum-wave-drag airfoil sections for arrow wings having the same airfoil sections at all spanwise stations. The drag of the wings was minimized subject to the condition of either a given thickness ratio at a specified chordwise location or a given volume. Numerical computations of the airfoil shape and wing wave drag were performed for a delta wing and for an arrow wing having a ratio of the tangent of the trailing-edge sweep angle to the tangent of the leading-edge sweep angle of 0.4. The range of the ratio of the tangent of the leading-edge sweep angle to the tangent of the Mach line sweep angle extended from 0 (two-dimensional) to 2.5.

INTRODUCTION

At supersonic speeds, the theoretical determination of minimum-wave-drag wings is of importance in establishing criteria for efficient aeronautical design. There is a rapidly increasing amount of information based on linear theory (refs. 1 to 4) and slender-body theory (refs. 5 and 6) to serve as a guide for the selection of three-dimensional minimum-wave-drag wings of given thickness or volume. As yet, however, little information exists for specifying the shapes for minimum-drag airfoil sections for wing plan forms of current interest at supersonic Mach numbers. It is the purpose of the present paper to study this problem by linearized theory.

A constant-thickness-ratio wing of arrow plan form with an arbitrary airfoil section is considered. For convenience, the root chord of the wing is assumed to be unity. The airfoil section (assumed to be the same at all spanwise stations) is composed of a series of straight-line segments. The drag of such a wing is then minimized subject to the restriction of either a given thickness ratio at a specified chordwise location or a given volume, and the equations for the corresponding minimum-drag airfoil shapes are determined. Computations are made to establish the minimum number of sides required for a reasonable determination of the airfoil shape and drag. Optimum sections and the corresponding wing drag coefficients are then calculated for a series of delta and arrow wings swept various amounts ahead of and behind the Mach lines. As a limiting case, the results of the optimum-airfoil calculations for a delta wing of fixed volume are compared with those of the corresponding airfoil derived analytically from slender-body theory.

The authors wish to acknowledge the coöperative efforts of the National Bureau of Standards personnel, particularly Otto Steiner, Sally Tsingou, and Norman Levine, who set up the coding and carried through the numerical computations on the National Bureau of Standards Eastern Automatic Computer during June 1953.

SYMBOLS

M	Mach number
β	cotangent of Mach angle, $\sqrt{M^2 - 1}$
t	thickness ratio
N	number of equally spaced straight-line segments used to form one side of symmetrical airfoil (number of chord divisions)
k	tangent of sweep angle of any arbitrary ridge line
k_1	tangent of sweep angle of leading edge
k_{N+1}	tangent of sweep angle of trailing edge
$n = k/\beta$	
x,y,z	Cartesian coordinates (see fig. 1)
A	cross-sectional area of body at station x
A_{max}	maximum cross-sectional area of body
λ	slope of airfoil surface divided by thickness ratio
$z(x)$	airfoil shape function
K	ratio of airfoil cross-sectional area to area of circumscribing rectangle
p	integer specifying last subsonic ridge line

m	integer specifying location of maximum thickness
i,j,r,α,β	arbitrary indices

$\Delta\lambda_r = \lambda_r - \lambda_{r-1}$

B',B,D,f	functions used to determine drag
F	function of $\Delta\lambda$ defined by equation (8)
C_D	drag coefficient based on wing area

ANALYSIS

Linear Theory

In reference 1, the basic equations for the drag of arrow wings of double-wedge airfoil sections have been obtained by the superposition of constant-strength source distributions within the wing plan form. This method has been extended in reference 7 into a generalized procedure whereby the wave drag of arrow wings having arbitrary profiles may be determined. This extension is accomplished by using a finite number of constant-strength source distributions and hence entails approximating the airfoil section by a multisided polygon. If the sides of the polygon are equally spaced (fig. 1) and the airfoil section is symmetrical, the drag at zero angle of attack is, in slightly different notation from that of reference 7,

$$\frac{N^2\pi\beta C_D}{8\left(1 - \frac{n_{N+1}}{n_1}\right)t^2} = -\sum_{i=1}^{p}\sum_{j=1}^{p}(j - i)^2\frac{n_1}{n_i}B'\left(n_i,\frac{n_j}{n_i}\right)\Delta\lambda_i\,\Delta\lambda_j - \sum_{i=1}^{p}\sum_{j=p+1}^{N+1}(j - i)^2\frac{n_1}{n_i}B\left(n_i,\frac{n_j}{n_i}\right)\Delta\lambda_i\,\Delta\lambda_j + \sum_{i=2}^{p}\sum_{j=1}^{i-1}\frac{n_1}{n_i}\left(\frac{n_i}{n_j}\right)^2(j - i)^2 D\left(n_i,\frac{n_i}{n_j}\right)\Delta\lambda_i\,\Delta\lambda_j - \sum_{i=p+1}^{N}\sum_{j=i+1}^{N+1}(j - i)^2\frac{n_1}{n_i}f\left(n_i,\frac{n_j}{n_i}\right)\Delta\lambda_i\,\Delta\lambda_j \tag{1}$$

where the new variable $\Delta\lambda_r$ is given by

$$\Delta\lambda_r = \lambda_r - \lambda_{r-1}$$

and where λ is defined by the relationship

$$\lambda = \frac{\frac{dz}{dx}}{t}$$

In equation (1), the index p defines the last subsonic ridge line (a subsonic line is one whose normal Mach number component is subsonic; see fig. 1) and has the integer value determined from

$$\frac{N(n_1 - 1)}{n_1 - n_{N+1}} + 1 > p \geqq \frac{N(n_1 - 1)}{n_1 - n_{N+1}} \tag{2}$$

The values of n are geometrically related by the equation

$$n_i = n_1 - \frac{i - 1}{N}(n_1 - n_{N+1}) \tag{3}$$

The formulas for the functions B', B, D, and f obtained from reference 7 are

$$B'\left(n_i,\frac{n_j}{n_i}\right) = \frac{1}{1 - \left(\frac{n_j}{n_i}\right)^2}\left[\frac{\log_e n_i}{\sqrt{n_i^2 - 1}} + \frac{n_j}{n_i}\,\frac{\cosh^{-1}n_i}{\sqrt{n_i^2 - 1}} + \right.$$

$$\left.\frac{1}{\sqrt{n_j^2 - 1}}\log_e\left(1 + \frac{2\sqrt{n_j^2 - 1}}{n_i - n_j + \sqrt{n_i^2 - 1} - \sqrt{n_j^2 - 1}}\right)\right] \tag{4a}$$

$$B\left(n_i, \frac{n_j}{n_i}\right) = \frac{1}{1 - \left(\frac{n_j}{n_i}\right)^2}\left[\frac{\log_e n_i}{\sqrt{n_i^2 - 1}} + \frac{n_j}{n_i}\,\frac{\cosh^{-1} n_i}{\sqrt{n_i^2 - 1}} + \right.$$

$$\left. \frac{2}{\sqrt{1 - n_j^2}} \tan^{-1}\left(\frac{\sqrt{1 - n_j^2}}{n_i - n_j + \sqrt{n_i^2 - 1}}\right)\right] \tag{4b}$$

$$D\left(n_i, \frac{n_i}{n_j}\right) = \frac{1}{1 - \left(\frac{n_i}{n_j}\right)^2}\left(\frac{\log_e n_i}{\sqrt{n_i^2 - 1}} + \right.$$

$$\left. \frac{1}{\sqrt{n_j^2 - 1}} \log_e \left\{\frac{n_i^2 - \frac{n_i}{n_j} + \sqrt{\left[n_i^2 - \left(\frac{n_i}{n_j}\right)^2\right]\left(n_i^2 - 1\right)}}{n_i\left(1 - \frac{n_i}{n_j}\right)}\right\}\right) \tag{4c}$$

$$f\left(n_i, \frac{n_j}{n_i}\right) = \frac{1}{1 - \left(\frac{n_j}{n_i}\right)^2}\left[\frac{\frac{n_j}{n_i}}{\sqrt{1 - n_i^2}} \cos^{-1} n_i + \frac{1}{\sqrt{1 - n_j^2}}\left(\frac{\pi}{2} + \sin^{-1} n_j\right)\right] \tag{4d}$$

In order to investigate optimum airfoil sections for arrow wings, the drag, as given by equation (1), is minimized subject to the specified thickness or volume condition and the airfoil shape parameters $\Delta\lambda_i$ are determined.

The specified conditions are:

(1) The airstream ahead of and behind the wing is parallel to the wing-chord plane

$$\phi_1 = \sum_{i=1}^{N+1} \Delta\lambda_i = 0 \tag{5}$$

(2) The airfoil must close at the leading and trailing edges

$$\phi_2 = \sum_{i=1}^{N+1} i\ \Delta\lambda_i = 0 \tag{6}$$

(3) The airfoil must have a given thickness ratio t at a specified fraction of the chord m/N

$$\phi_{3a} = 2\sum_{i=1}^{m} (m + 1 - i)\Delta\lambda_i - N = 0 \tag{7a}$$

or the airfoil must have a given cross-sectional area so that the wing has a given volume

$$\phi_{3b} = \frac{1}{N^2}\sum_{i=1}^{N+1} i^2\Delta\lambda_i - K = 0 \tag{7b}$$

In equation (7b), K specifies the ratio of the cross-sectional area of the optimum airfoil to the area of the circumscribing rectangle (a point discussed subsequently).

The shape of the minimum-drag airfoil can be obtained analytically by the extreme-value theory of reference 8. Since the thickness distribution $z(x)/t$ of an optimum airfoil section is independent of the thickness ratio (a fact that can be inferred from eq. (1)), the minimum-drag shapes are determined by first formulating the function

$$F = \frac{\pi N^2}{8\left(1 - \frac{n_{N+1}}{n_1}\right)}\frac{\beta C_D}{t^2} + X\phi_1 + Y\phi_2 + Z\begin{Bmatrix}\phi_{3a}\\ \phi_{3b}\end{Bmatrix}^{*} \tag{8}$$

---

*The braces indicate that the appropriate condition, either ϕ_{3a} or ϕ_{3b}, is used.

where $\dfrac{\pi N^2}{8\left(1 - \dfrac{n_{N+1}}{n_1}\right)} \dfrac{\beta C_D}{t^2}$ is the function of $\Delta\lambda$ specified by equation (1) and ϕ_1, ϕ_2, ϕ_{3a}, and ϕ_{3b} are the functions of $\Delta\lambda$ specified by equations (5), (6), (7a), and (7b), respectively. The variables X, Y, and Z are undetermined multipliers. The optimum $\Delta\lambda$ values are then obtained by solving the system of $N + 4$ linear simultaneous algebraic equations given by:

$$\frac{\partial F}{\partial \Delta\lambda_r} = 0 \tag{9}$$

$$\phi_1 = 0 \tag{10}$$

$$\phi_2 = 0 \tag{11}$$

and either

$$\phi_{3a} = 0 \tag{12a}$$

or

$$\phi_{3b} = 0 \tag{12b}$$

Equations (9) to (12) are shown in matrix notation in exploded form in figure 2; the relations for the individual entries in the matrix are also included. The interchange of the area condition for the thickness condition simply changes one row and one column of the matrix as indicated in figure 2.

In the numerical evaluation of the optimum airfoil for a specified area, the parameter K depends upon the airfoil shape. The calculated values of $\Delta\lambda$, however, are directly proportional to any assumed value of K. Hence, any arbitrary value may be initially selected and the solution linearly scaled so that the relationship for the airfoil coordinates

$$z_r = 2z_{r-1} - z_{r-2} + \frac{t\ \Delta\lambda_{r-1}}{N} \tag{13}$$

yields a value of z_r/t equal to 0.5 at the location of maximum thickness.

Slender-Body Theory

In reference 6, it is established, on the basis of slender-body theory, that the optimum wing and body of revolution (both for a given length and volume) have the same axial cross-sectional area distribution. Hence, as a limiting case for n arbitrarily large, the airfoil section obtained by this slender-body method can be compared with the results of the previous linear analysis.

The shape of the airfoil section of a constant-thickness-ratio delta wing having the same axial cross-sectional area distribution as a body of revolution is

$$\frac{z(x)}{t} = \frac{1}{2} \frac{(1 - x)\frac{dA(x)}{dx} + 2A(x)}{\left(1 - x_{max}\right)\left[\frac{dA(x)}{dx}\right]_{x=x_{max}} + 2A\left(x_{max}\right)} \tag{14}$$

where x_{max} is the location of maximum thickness of the airfoil and $A(x)$ is the axial cross-sectional area distribution of the body or wing. Equation (14), when applied to the minimum-drag body of revolution for a given length and volume (ref. 9)

$$\frac{A(x)}{A_{max}} = 8(x - x^2)^{3/2} \tag{15}$$

results in the airfoil shape

$$\frac{z(x)}{t} = \frac{1}{2} \frac{(x - x^2)^{1/2}(2x - 3)(x - 1)}{\left(x_{max} - x_{max}^2\right)^{1/2}\left(2x_{max} - 3\right)\left(x_{max} - 1\right)} \tag{16}$$

where $x_{max} = \dfrac{3 - \sqrt{5}}{4}$.

The shape determined by equation (16) is compared with the linear-theory shapes in the following section.

NUMERICAL RESULTS

Effect of number of sides N.- The initial problem consisted in establishing the number of sides per surface N required for a reasonable approximation to the shape and drag of the limiting airfoil having an infinite number of sides. For this trial calculation a delta wing was assumed and the thickness condition applied. A location of maximum thickness m/N of 0.20 of the chord was selected and a value of $n_1 = 1.7$ (subsonic leading edge) was assumed. A subsonic-leading-edge condition was selected since it was anticipated that the limiting airfoil would have a round nose and hence require the largest number of flat sides per surface N for a good approximation.

The results of the computations for $N = 5$, 10, 20, and 40 sides are shown in figure 3 and presented in table I. Perhaps more striking in figure 3 than the influence of the number of sides is the bump located at the position of maximum thickness. From an examination of all the numerical computations, it can be inferred that this bump, which tends to become more cusplike as the number of sides increases, occurs only when the thickness auxiliary condition is applied with a subsonic maximum-thickness line. For such conditions, the resulting airfoil is in violation of the assumptions of linearized theory and hence represents a restriction on the use of such a theory. Furthermore, in the use of such airfoils, flow separation would undoubtedly be a governing factor. As is demonstrated subsequently, if the maximum-thickness line is supersonic or if the area condition is used, no such difficulty arises. From figure 3, it can be seen that an increase in the number of sides from 20 to 40 has little effect on either the drag or the airfoil shape; a value of $N = 20$ was therefore selected for all succeeding computations. Since in this test case the limiting airfoil appears to be a difficult one to approximate by line segments, it is believed that the value of $N = 20$ is entirely adequate.

Range of computations.- The computations of the wave drag and airfoil shape for the optimum airfoil sections were performed for delta wings and for arrow wings, that is, wings having a ratio of the tangent of the trailing-edge sweep angle to the tangent of the leading-edge sweep angle of 0 and 0.4, respectively. The range of values of n_1 extended from 0.5 to 2.5. For the thickness condition, maximum-thickness locations of 0.20 and 0.50 of the chord were investigated. A complete summary of the range of computations is presented in table II. The final computations are tabulated in tables III and IV for the delta and arrow plan forms, respectively, and are plotted in figures 4 and 5. Figures 4 and 5 also include the two-dimensional ($n_1 = 0$) optimum results.

Optimum section for the thickness condition.- Figure 4 presents a comparison of the optimum-airfoil-shape and drag calculations with corresponding double-wedge results (ref. 10) for two chordwise locations of maximum thickness: 0.20 and 0.50. For the 0.20 location of maximum thickness (fig. 4(a)) all results for $n_1 > 1$ correspond to subsonic maximum-thickness lines; whereas for the 0.50 location (fig. 4(b)) all results correspond to supersonic maximum-thickness lines.

For both locations of maximum thickness (figs. 4(a) and 4(b)), plan form has little effect on the optimum shapes. For $n_1 \leqq 1$ the optimum airfoil has almost the same shape and drag as the double-wedge airfoil (figs. 4(a) and 4(b)). For the 0.50 location of maximum thickness (fig. 4(b)), both wings have, for subsonic leading edges ($n_1 > 1$), optimum sections which are more full at the front, more closely resemble subsonic airfoils, and have about 16 percent less drag than the corresponding double-wedge section. For the 0.20 location of maximum thickness (fig. 4(a)), the progressive decrease in magnitude of the bump at maximum thickness is apparent as n_1 decreases. No discussion of the drag of wings having subsonic maximum-thickness lines is considered to be warranted in view of the limitations on the theory and the separation problem in a real flow for this case.

Optimum section for the area condition.- Figure 5 presents the drag and optimum airfoil shapes for delta and arrow wings of a given volume. Again the airfoil shapes are plotted at the appropriate n_1 values. As was the result for the thickness condition, plan form had little effect on the optimum section, and for the supersonic leading edges, the two-dimensional optimum (the biconvex section) results for all practical purposes. This latter result was established for an elliptic-plan-form wing in reference 3. For subsonic leading edges ($n_1 > 1$), the airfoils become more full at the front and again resemble subsonic airfoils. The maximum-thickness location has moved forward for large values of n_1 and for the last case computed occurs at 25 percent of the chord. The progressive rounding of the nose section of the delta wing for highly subsonic leading edges is shown in figure 6 where the slender-body airfoil ($n_1 \rightarrow \infty$) given by equation (16) (table V) is compared with airfoils derived from linear theory. For this slender-body airfoil, the location of maximum thickness is at 19 percent of the chord. For a value of n_1 of 2.5 the linearized result already indicates a close similarity with the limiting result ($n_1 \rightarrow \infty$) as obtained by slender-body theory.

The optimum linear-theory airfoil, subject to the thickness condition, is not compared with the slender-body airfoil (derived from an optimum body of given length and diameter) because the auxiliary conditions are not comparable.

Comparison of airfoil sections for wings of given volume.- In order to establish a basis of comparison for the drag results in figure 5, the drag of wings of the same plan form and volume but having biconvex and

NACA 65A-series sections was calculated (again for $N = 20$) and is compared in figure 7 with the drag of optimum sections. This comparison is, perhaps, somewhat artificial in that preselected values of the location of maximum thickness exist for the biconvex (50 percent) and the NACA 65A-series (40 percent) wings. These results are believed to be of interest, however, inasmuch as the biconvex section is the two-dimensional ($n_1 = 0$) optimum for a given area and the 65A-series section is of current interest.

For the supersonic leading edges, the drag reduction of the optimum section as compared with that for the biconvex section is small and amounts to less than 10 percent. For the subsonic leading edges, the drag reduction of the optimum section is 25 percent of that of the biconvex wing of delta plan form and 33 percent of that of arrow plan form for a value of n_1 of 1.7 (60° leading-edge sweep at $M = 1.4$, for example). Corresponding values of the drag reduction of the optimum section as compared with those for the NACA 65A-series sections would be about 10 percent and 15 percent, respectively, at the same value of n_1.

CONCLUSIONS

A linearized theoretical analysis has been made to determine the minimum-wave-drag airfoil sections for arrow wings having the same airfoil sections at all spanwise stations. The drag of the wings was minimized subject to the condition of either a given thickness ratio at a specified chordwise location or a given volume. Numerical computations were performed for a delta wing and an arrow wing having a ratio of the tangent of trailing-edge sweep angle to the tangent of the leading-edge sweep angle of 0.4. The results of the computations indicate that:

1. For either the thickness or the volume condition:

   (a) The change in plan form resulted in only a slight change in the optimum section for either subsonic or supersonic leading edges.

   (b) The optimum airfoil section for supersonic leading edges is very nearly the two-dimensional optimum and the drag reduction from the two-dimensional optimum is less than 10 percent.

2. For the thickness condition:

   (a) Drag reductions of about 16 percent from double-wedge sections resulted for two examples having subsonic leading edges and supersonic maximum-thickness lines located at 50 percent of the chord.

(b) The optimum airfoil sections obtained for subsonic leading edges with subsonic maximum-thickness lines violate the assumptions of linear theory. Flow separation over these airfoils would be a governing factor in the drag determination.

3. For the volume condition:

(a) Drag reductions of 25 percent and 33 percent from biconvex sections resulted for a delta wing and an arrow wing, respectively, for a 60° swept leading edge at a Mach number of 1.4. When compared with NACA 65A-series sections for the same conditions, the drag reduction is about 10 percent and 15 percent, respectively.

(b) The optimum airfoil section for a very slender delta wing obtained by this analysis approaches the slender-body optimum section.

Langley Aeronautical Laboratory,
National Advisory Committee for Aeronautics,
Langley Field, Va., February 17, 1954.

REFERENCES

1. Puckett, Allen E.: Supersonic Wave Drag of Thin Airfoils. Jour. Aero. Sci., vol. 13, no. 9, Sept. 1946, pp. 475-484.

2. Jones, Robert T.: The Minimum Drag of Thin Wings in Frictionless Flow. Jour. Aero. Sci., vol. 18, no. 2, Feb. 1951, pp. 75-81.

3. Jones, Robert T.: Theoretical Determination of the Minimum Drag of Airfoils at Supersonic Speeds. Jour. Aero. Sci., vol. 19, no. 12, Dec. 1952, pp. 813-822.

4. Graham, E. W.: A Drag Reduction Method for Wings of Fixed Plan Form. Jour. Aero. Sci., vol. 19, no. 12, Dec. 1952, pp. 823-825.

5. Adams, Mac C., and Sears, W. R.: Slender-Body Theory - Review and Extension. Jour. Aero. Sci., vol. 20, no. 2, Feb. 1953, pp. 85-98.

6. Heaslet, Max. A., and Lomax, Harvard: The Calculation of Pressure on Slender Airplanes in Subsonic and Supersonic Flow. NACA TN 2900, 1953.

7. Beane, Beverly: The Characteristics of Supersonic Wings Having Biconvex Sections. Jour. Aero. Sci., vol. 18, no. 1, Jan. 1951, pp. 7-20.

8. Courant, R.: Differential and Integral Calculus. Vol. II. Nordemann Publishing Co., Inc. (New York), 1940, pp. 183-199.

9. Lighthill, M. J.: Supersonic Flow Past Bodies of Revolution. R. & M. No. 2003, British A.R.C., 1945.

10. Puckett, A. E., and Stewart, H. J.: Aerodynamic Performance of Delta Wings at Supersonic Speeds. Jour. Aero. Sci., vol. 14, no. 10, Oct. 1947, pp. 567-578.

TABLE I.- DELTA-WING AIRFOIL ORDINATES z/t AND DRAG PARAMETERS

$\left[n = 1.7; \frac{m}{N} = 0.2\right]$

x	Ordinate, z/t			
	N = 5	N = 10	N = 20	N = 40
0	0	0	0	0
.025	------	-------	-------	.11060
.050	------	-------	.17084	.15093
.075	------	-------	-------	.18862
.100	------	.24812	.24078	.22154
.125	------	-------	-------	.25309
.150	------	-------	.29181	.28982
.175	------	-------	-------	.31681
.200	.5000	.50000	.50000	.50000
.225	------	-------	-------	.31175
.250	------	-------	.29533	.28663
.275	------	-------	-------	.26085
.300	------	.28241	.26651	.24394
.325	------	-------	-------	.23050
.350	------	-------	.23900	.21936
.375	------	-------	-------	.20966
.400	.2818	.24246	.21935	.20089
.425	------	-------	-------	.19248
.450	------	-------	.20106	.18414
.475	------	-------	-------	.17584
.500	------	.20226	.18297	.16759
.525	------	-------	-------	.15934
.550	------	-------	.16497	.15110
.575	------	-------	-------	.14286
.600	.1852	.16243	.14695	.13460
.625	------	-------	-------	.12633
.650	------	-------	.12887	.11804
.675	------	-------	-------	.10974
.700	------	.12236	.11071	.10140
.725	------	-------	-------	.09305
.750	------	-------	.09247	.08468
.775	------	-------	-------	.07628
.800	.0930	.08193	.07413	.06787
.825	------	-------	-------	.05943
.850	------	-------	.05571	.05098
.875	------	-------	-------	.04251
.900	------	.04113	.03721	.03402
.925	------	-------	-------	.02551
.950	------	-------	.01864	.01699
.975	------	-------	-------	.00845
1.000	0	0	0	.00010
$\frac{\beta C_D}{t^2}$	2.337	2.0677	1.8412	1.6745

TABLE II.- RANGE OF COMPUTATIONS FOR OPTIMUM AIRFOIL CALCULATIONS

[N = 20]

k_{N+1}/k_1	n	Thickness condition, $\frac{m}{N} = 0.2$	Thickness condition, $\frac{m}{N} = 0.5$	Area condition
0	0.5	x	x	x
	1.0	x	x	x
	1.3	x		x
	1.7	x	x	x
	2.5			x
.4	.5	x	x	x
	1.3		x	x
	1.7	x		x
	2.5	x		x

TABLE III.- DELTA-WING AIRFOIL ORDINATES z/t AND DRAG PARAMETERS

$[k_{N+1}/k_1 = 0;\ N = 20]$

(a) Thickness condition

x	Ordinate, z/t						
	$n_1 = 0.5$		$n_1 = 1.0$		$n_1 = 1.3$	$n_1 = 1.7$	
	$\frac{m}{N} = 0.2$	$\frac{m}{N} = 0.5$	$\frac{m}{N} = 0.2$	$\frac{m}{N} = 0.5$	$\frac{m}{N} = 0.2$	$\frac{m}{N} = 0.2$	$\frac{m}{N} = 0.5$
0	0	0	0	0	0	0	0
.05	.12232	.04730	.09318	.03178	.26726	.17084	.18773
.10	.24647	.09527	.21704	.07379	.36301	.24078	.25347
.15	.37238	.14386	.35377	.11981	.43763	.29181	.31108
.20	.50000	.19305	.50000	.16856	.50000	.50000	.35683
.25	.46986	.24283	.48909	.21948	.46787	.29533	.39527
.30	.43951	.29317	.47172	.27227	.44557	.26651	.42737
.35	.40897	.34407	.44971	.32676	.42145	.23900	.45355
.40	.37826	.39551	.42423	.38289	.39516	.21935	.47170
.45	.34739	.44749	.39605	.44063	.36709	.20106	.48574
.50	.31637	.50000	.36571	.50000	.33756	.18297	.50000
.55	.28522	.45053	.33362	.45465	.30684	.16497	.46322
.60	.25393	.40091	.30007	.40778	.27512	.14695	.42034
.65	.22253	.35117	.26531	.35966	.24259	.12887	.37368
.70	.19102	.30131	.22953	.31047	.20935	.11071	.32440
.75	.15940	.25133	.19286	.26037	.17552	.09247	.27318
.80	.12769	.20125	.15544	.20949	.14119	.07413	.22047
.85	.09589	.15107	.11736	.15793	.10641	.05571	.16660
.90	.06400	.10080	.07872	.10578	.07126	.03721	.11179
.95	.03204	.05044	.03958	.05311	.03577	.01864	.05621
1.00	0	0	0	0	0	0	0
$\frac{\beta C_D}{t^2}$	6.9175	4.2211	10.4928	4.8363	4.7317	1.8412	3.5906

(b) Area condition

x	Ordinate, z/t				
	$n_1 = 0.5$	$n_1 = 1.0$	$n_1 = 1.3$	$n_1 = 1.7$	$n_1 = 2.5$
	K = 0.66312	K = 0.64093	K = 0.72793	K = 0.72200	K = 0.65085
0	0	0	0	0	0
.05	.08989	.05477	.26700	.33747	.35186
.10	.17165	.12292	.33477	.41427	.42793
.15	.24496	.19158	.38351	.46648	.47809
.20	.30952	.25707	.41485	.49090	.49771
.25	.36507	.31722	.44063	.50000	.50000
.30	.41137	.37051	.46392	.49903	.49020
.35	.44820	.41577	.48221	.49191	.47215
.40	.47536	.45206	.49448	.48194	.44853
.45	.49268	.47861	.50000	.47126	.42134
.50	.50000	.49477	.49818	.45789	.39218
.55	.49718	.50000	.48853	.44018	.36229
.60	.48410	.49383	.47063	.41732	.33311
.65	.46065	.47587	.44412	.38869	.30380
.70	.42673	.44580	.40872	.35384	.27223
.75	.38227	.40335	.36419	.31243	.23739
.80	.32720	.34832	.31035	.26419	.19873
.85	.26147	.28055	.24707	.20891	.15586
.90	.18504	.19994	.17426	.14649	.10853
.95	.09789	.10642	.09190	.07685	.05659
1.00	0	0	0	0	0
$\frac{\beta C_D}{t^2}$	5.6416	6.3176	5.1339	3.7968	2.1993

TABLE IV.- ARROW-WING AIRFOIL ORDINATES z/t AND DRAG PARAMETERS

$\left[k_{N+1}/k_1 = 0.4;\ N = 20\right]$

(a) Thickness condition

x	Ordinate, z/t				
	$n_1 = 0.5$		$n_1 = 1.3$	$n_1 = 1.7$	$n_1 = 2.5$
	$\frac{m}{N} = 0.2$	$\frac{m}{N} = 0.5$	$\frac{m}{N} = 0.5$	$\frac{m}{N} = 0.2$	$\frac{m}{N} = 0.2$
0	0	0	0	0	0
.05	.12328	.04813	.18765	.12491	.10972
.10	.24772	.09669	.25406	.18539	.16735
.15	.37330	.14569	.31204	.23191	.21306
.20	.50000	.19510	.35780	.50000	.50000
.25	.46993	.24493	.39558	.23220	.21435
.30	.43968	.29516	.42626	.19816	.17926
.35	.40925	.34579	.44993	.16201	.14075
.40	.37866	.39680	.46717	.13837	.11593
.45	.34790	.44821	.48367	.11955	.09633
.50	.31698	.50000	.50000	.10405	.08042
.55	.28591	.45092	.46569	.09076	.06700
.60	.25469	.40162	.42533	.07904	.05541
.65	.22333	.35211	.38070	.06847	.04520
.70	.19182	.30240	.33278	.05864	.03610
.75	.16018	.25248	.28218	.04889	.02790
.80	.12840	.20236	.22933	.03919	.02049
.85	.09649	.15206	.17450	.02948	.01379
.90	.06445	.10156	.11791	.01974	.00791
.95	.03229	.05087	.05971	.00992	.00250
1.00	0	0	0	0	0
$\frac{\beta C_D}{t^2}$	7.0034	4.3106	4.5221	0.9622	0.4710

(b) Area condition

x	Ordinate, z/t			
	$n_1 = 0.5$	$n_1 = 1.3$	$n_1 = 1.7$	$n_1 = 2.5$
	K = 0.66423	K = 0.73780	K = 0.63403	K = 0.60363
0	0	0	0	0
.05	.09106	.33391	.34183	.33808
.10	.17346	.41124	.41930	.41561
.15	.24702	.46394	.47227	.46966
.20	.31154	.48917	.49504	.49375
.25	.36686	.49934	.50000	.50000
.30	.41282	.50000	.49189	.49288
.35	.44925	.49552	.47425	.47572
.40	.47602	.48965	.44963	.45084
.45	.49298	.48232	.42000	.42000
.50	.50000	.47121	.38704	.38461
.55	.49697	.45526	.35219	.34581
.60	.48376	.43373	.31681	.30458
.65	.46027	.40601	.28220	.26177
.70	.42639	.37156	.24938	.21816
.75	.38203	.32993	.21600	.17450
.80	.32710	.28067	.18032	.13158
.85	.26151	.22340	.14148	.09021
.90	.18518	.15776	.09882	.05222
.95	.09803	.08340	.05182	.01630
1.00	0	0	0	0
$\frac{\beta C_D}{t^2}$	5.7462	4.9891	2.4748	1.3412

TABLE V.- DELTA-WING AIRFOIL ORDINATES BASED ON

SLENDER-BODY THEORY

x	z/t
0	0
.05	.36060
.10	.45403
.15	.49215
[a].19	.50000
.20	.49967
.25	.48760
.30	.46236
.35	.42825
.40	.38837
.45	.34509
.50	.30028
.55	.25546
.60	.21184
.65	.17044
.70	.13210
.75	.09752
.80	.06726
.85	.04182
.90	.02162
.95	.00720
1.00	0

[a]0.190983.

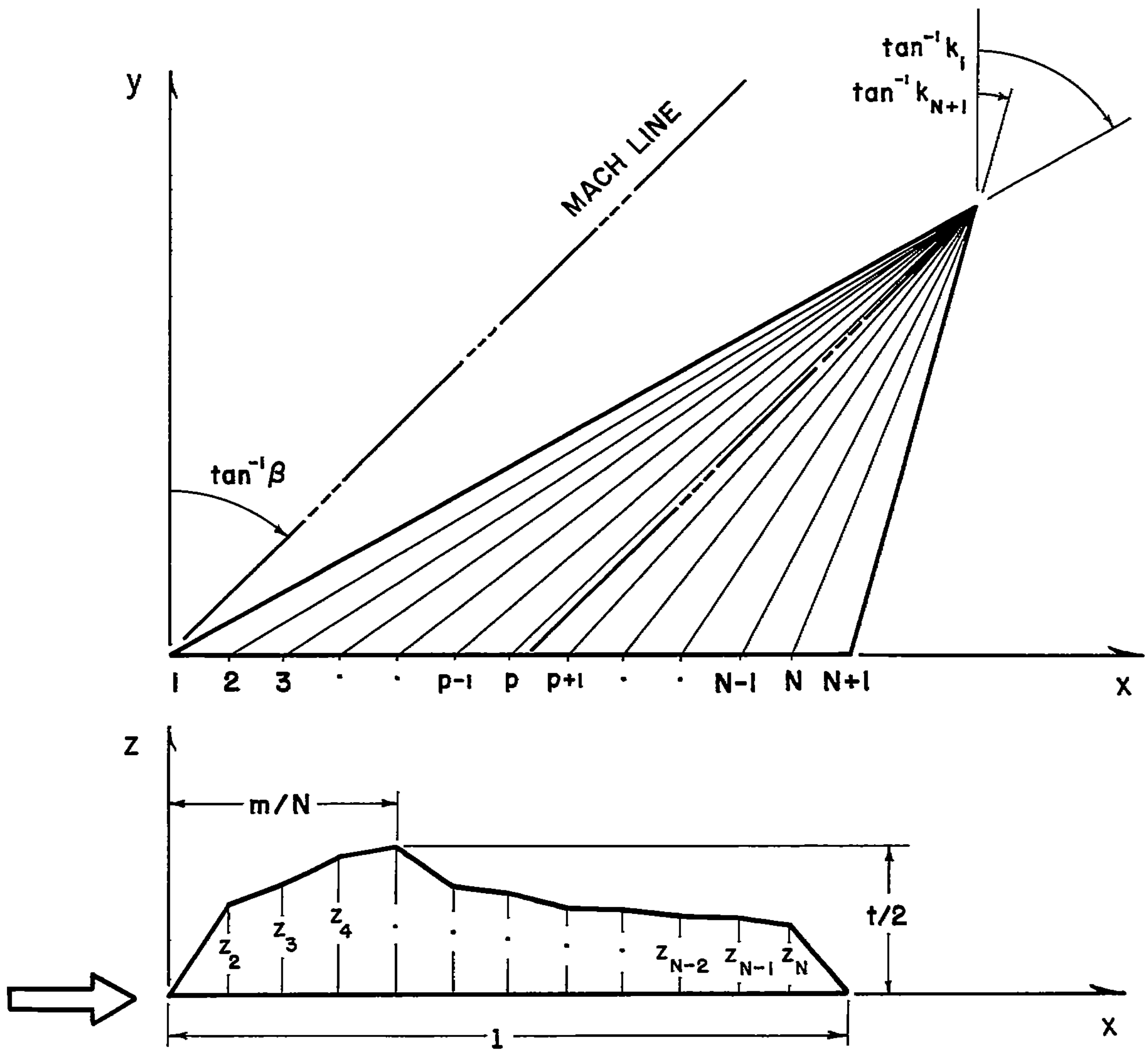

Figure 1.- Schematic drawing of wing geometry.

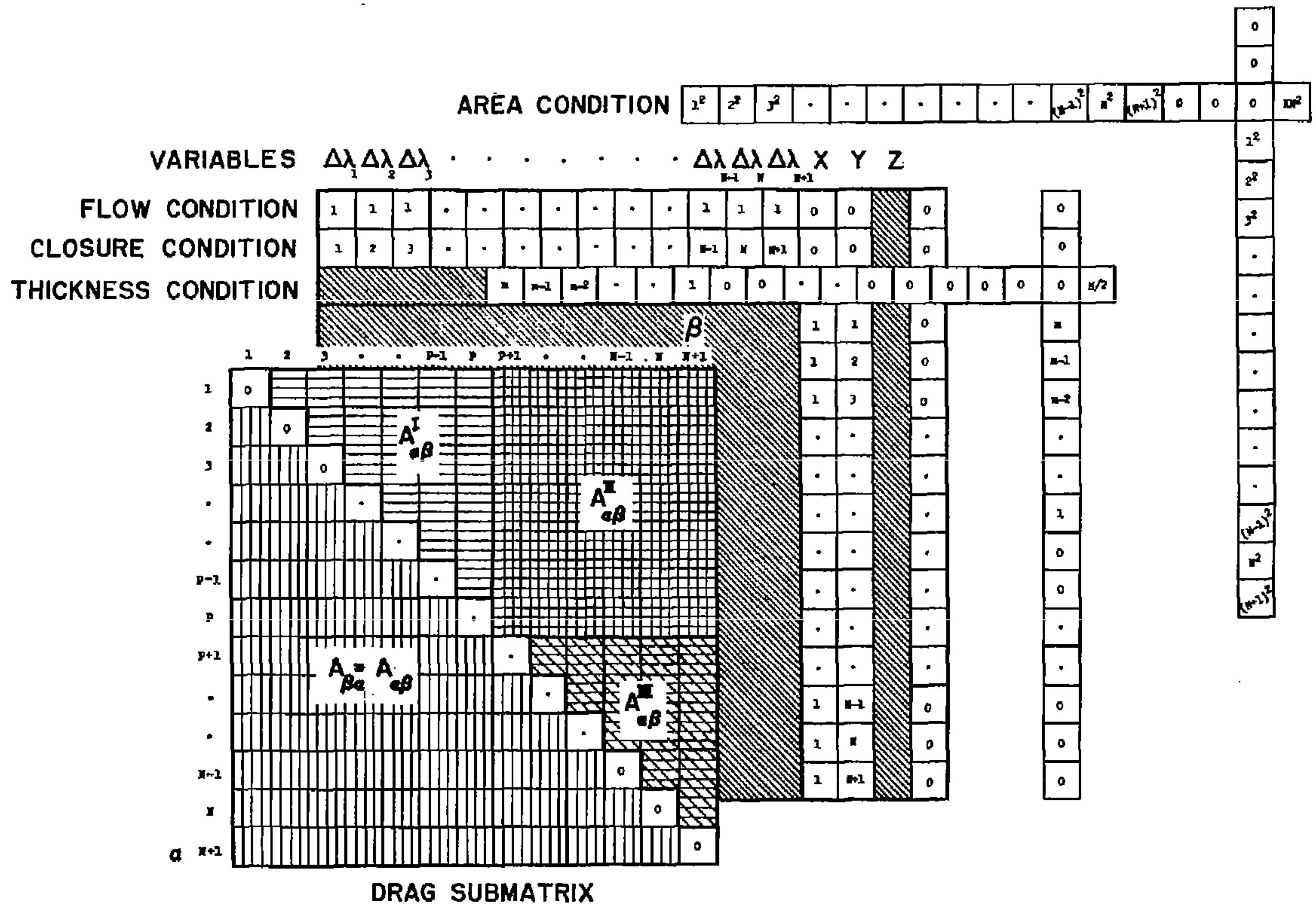

$$A^{I}_{\alpha\beta} = -(\alpha-\beta)^2 \frac{k_1}{k_\alpha} B'\left(n_\alpha, \frac{n_\beta}{n_\alpha}\right) + (\alpha-\beta)^2 \frac{k_1}{k_\beta}\left(\frac{k_\beta}{k_\alpha}\right)^2 D\left(n_\beta, \frac{n_\beta}{n_\alpha}\right) \qquad A^{II}_{\alpha\beta} = -(\alpha-\beta)^2 \frac{k_1}{k_\alpha} B\left(n_\alpha, \frac{n_\beta}{n_\alpha}\right) \qquad A^{III}_{\alpha\beta} = -(\alpha-\beta)^2 \frac{k_1}{k_\alpha} f\left(n_\alpha, \frac{n_\beta}{n_\alpha}\right)$$

Figure 2.- Exploded view of coefficient matrix of equations (9) to (12).

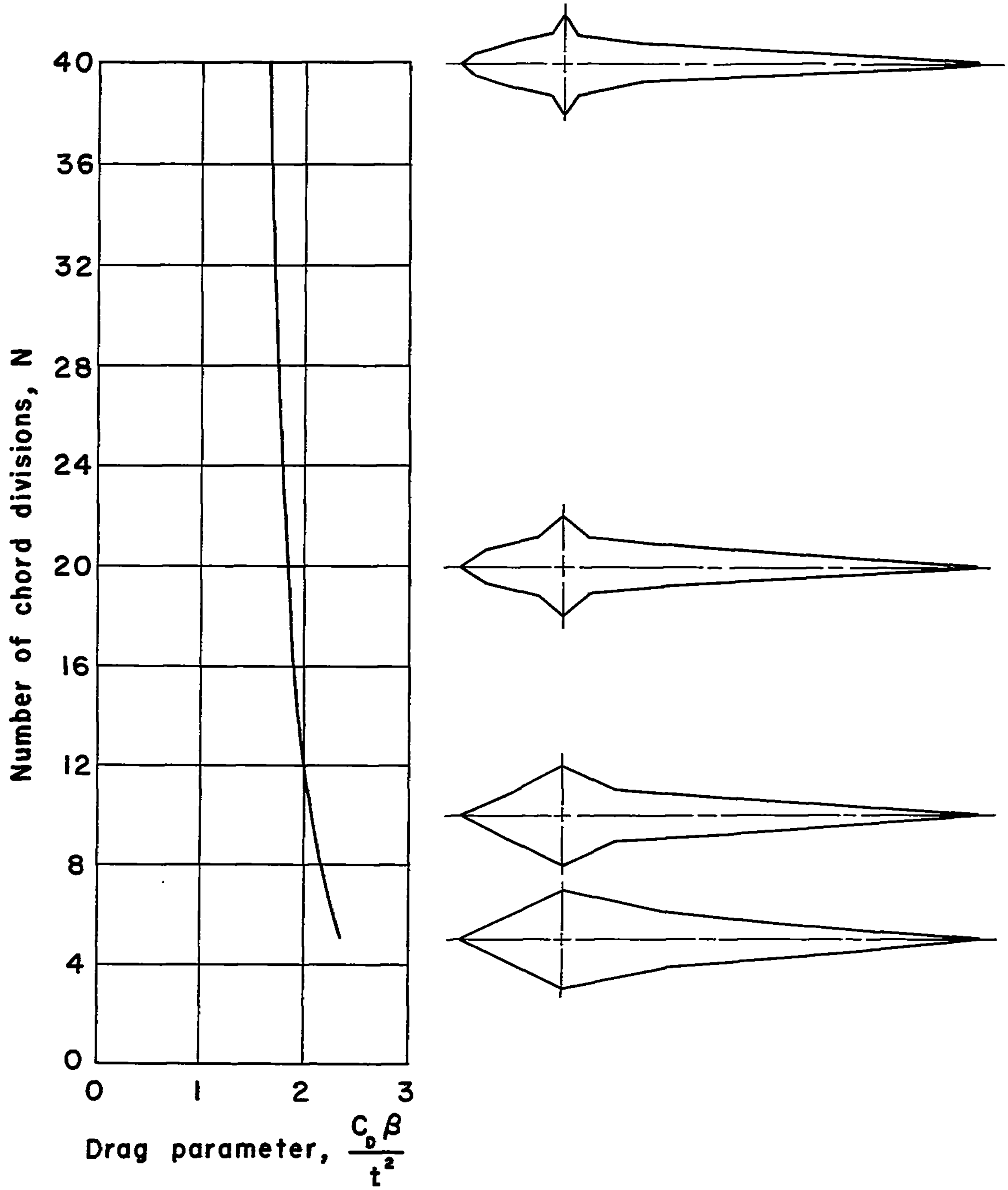

Figure 3.- Effect of number of chord divisions N on the drag and airfoil shapes of optimum delta wings. Thickness condition; $n_1 = 1.7$; $m/N = 0.20$.

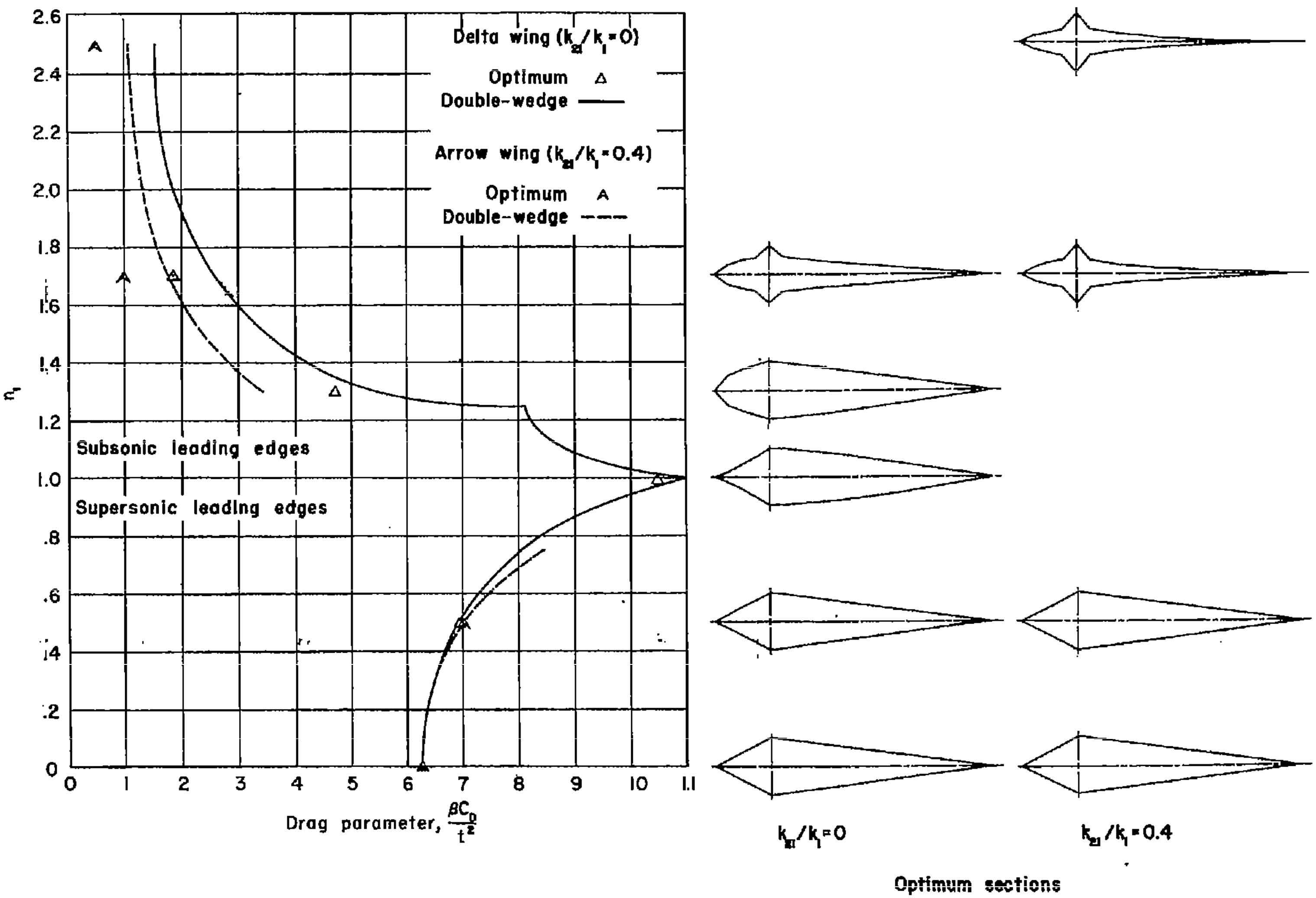

(a) m/N = 0.20.

Figure 4.- Wave drag and airfoil shapes of optimum delta and arrow wings. Thickness condition; N = 20.

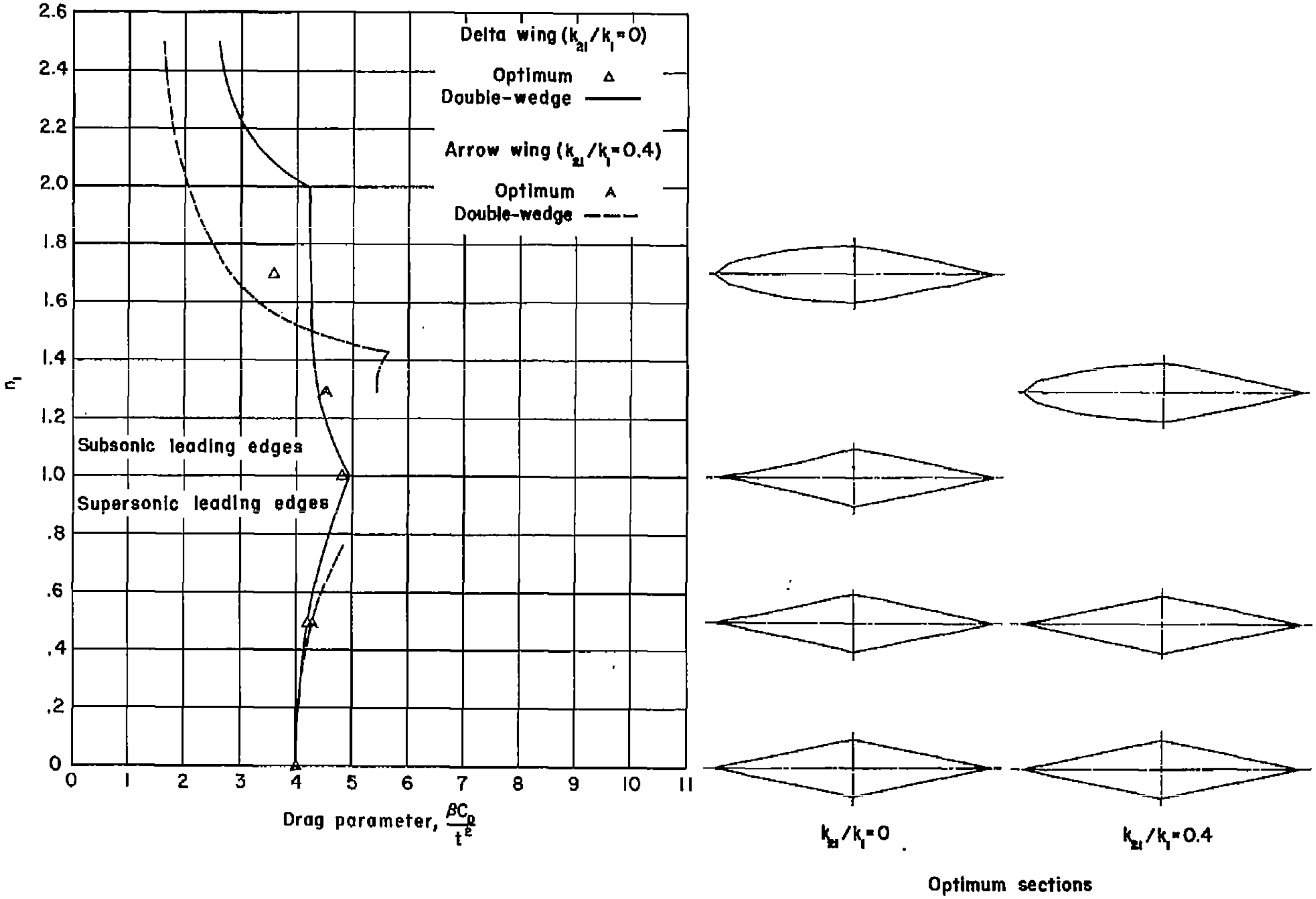

(b) m/N = 0.50.

Figure 4.- Concluded.

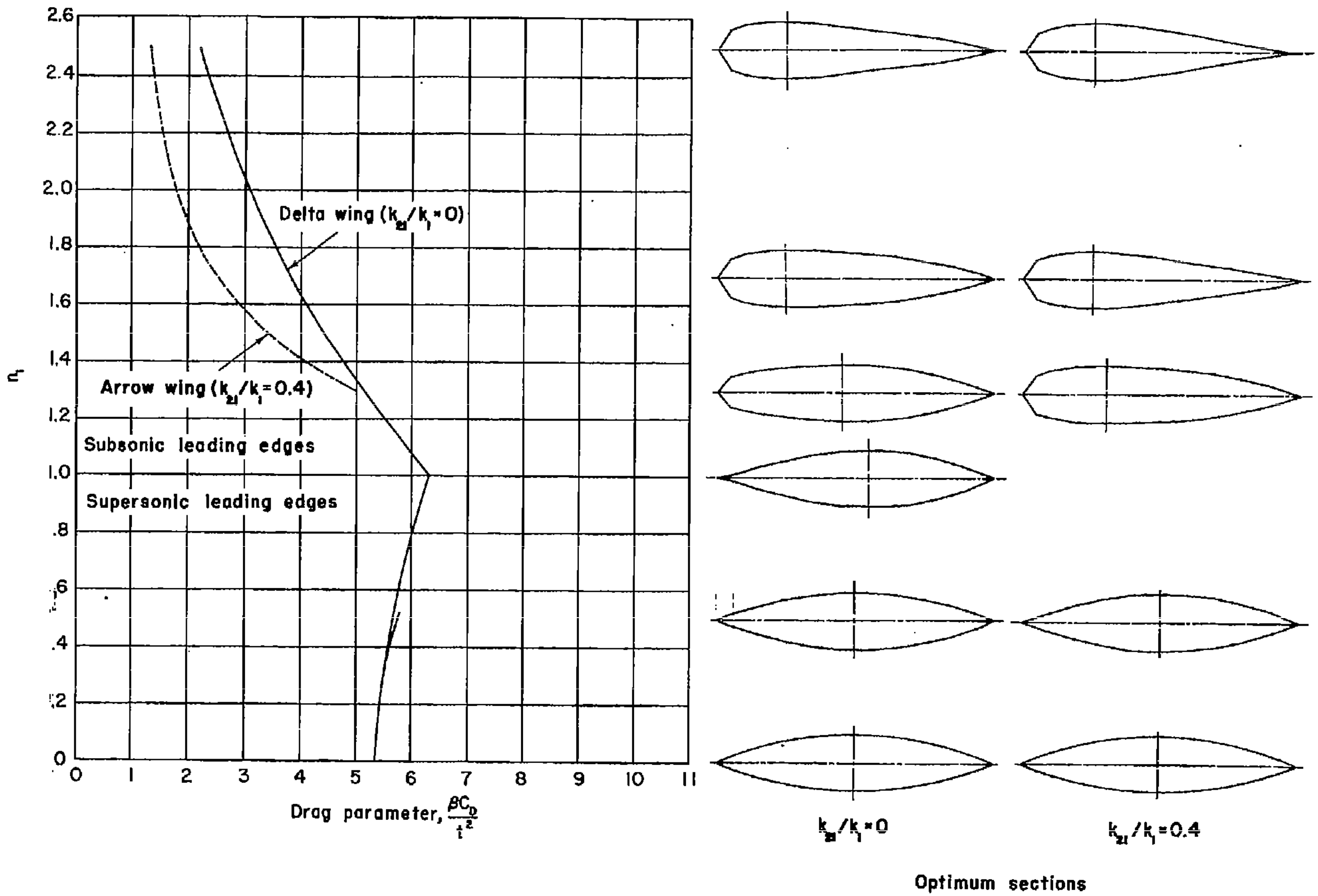

Figure 5.- Wave drag and airfoil shapes of optimum delta and arrow wings. Area condition; N = 20.

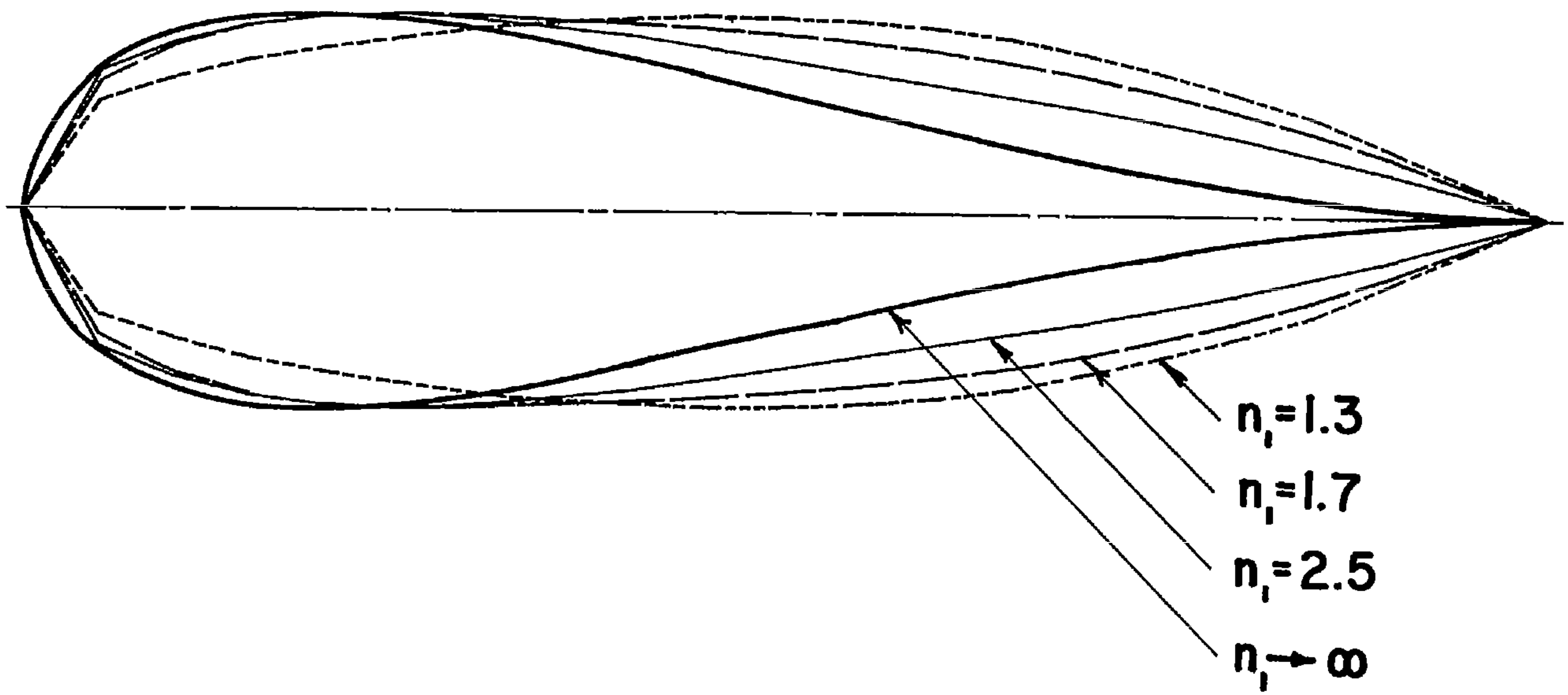

Figure 6.- Comparison of airfoil shapes for delta wings of given volume, as derived from linear theory and slender-body theory.

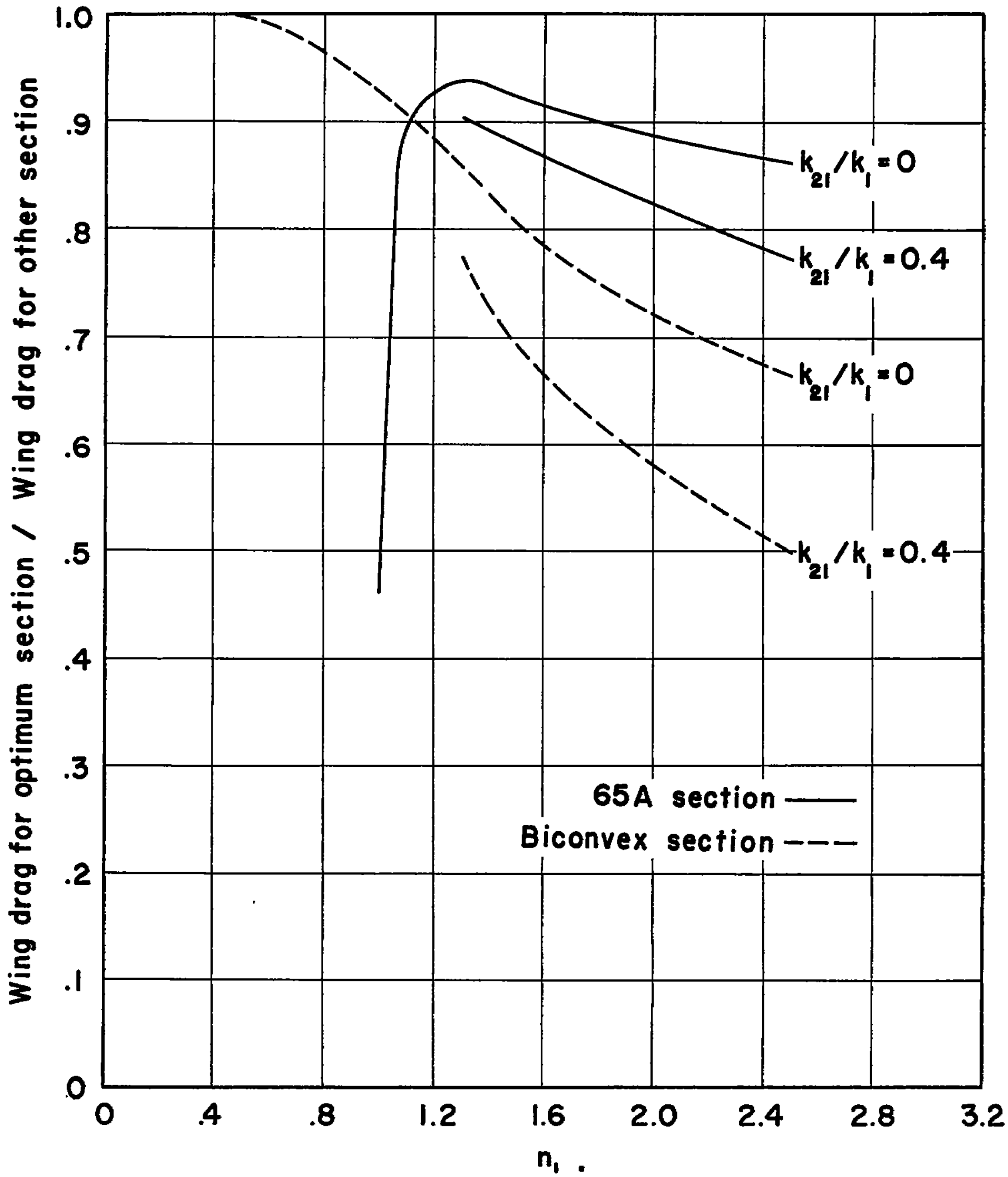

Figure 7.- Relative drags for optimum wings of given volume and wings of other sections and the same volume. N = 20.

NACA-Langley - 5-6-54 - 1000